General circulation model simulations of recent cooling in the east-central United States

Walter A. Robinson
Department of Atmospheric Sciences, University of Illinois at Urbana-Champaign, Urbana, Illinois, USA

Reto Reudy and James E. Hansen
NASA/Goddard Institute for Space Studies, New York, New York, USA

Received 10 December 2001; revised 30 April 2002; accepted 1 May 2002; published 19 December 2002.

[1] In ensembles of retrospective general circulation model (GCM) simulations, surface temperatures in the east-central United States cool between 1951 and 1997. This cooling, which is broadly consistent with observed surface temperatures, is present in GCM experiments driven by observed time varying sea-surface temperatures (SSTs) in the tropical Pacific, whether or not increasing greenhouse gases and other time varying climate forcings are included. Here we focus on ensembles with fixed radiative forcing and with observed varying SST in different regions. In these experiments the trend and variability in east-central U.S. surface temperatures are tied to tropical Pacific SSTs. Warm tropical Pacific SSTs cool U.S. temperatures by diminishing solar heating through an increase in cloud cover. These associations are embedded within a year-round response to warm tropical Pacific SST that features tropospheric warming throughout the tropics and regions of tropospheric cooling in midlatitudes. Precipitable water vapor over the Gulf of Mexico and the Caribbean and the tropospheric thermal gradient across the Gulf Coast of the United States increase when the tropical Pacific is warm. In observations, recent warming in the tropical Pacific is also associated with increased precipitable water over the southeast United States. The observed cooling in the east-central United States, relative to the rest of the globe, is accompanied by increased cloud cover, though year-to-year variations in cloud cover, U.S. surface temperatures, and tropical Pacific SST are less tightly coupled in observations than in the GCM. *INDEX TERMS:* 1620 Global Change: Climate dynamics (3309); 1610 Global Change: Atmosphere (0315, 0325); 3309 Meteorology and Atmospheric Dynamics: Climatology (1620); 3339 Meteorology and Atmospheric Dynamics: Ocean/atmosphere interactions (0312, 4504); *KEYWORDS:* global warming, U.S. climate, global climate model (GCM), sea surface temperature, cloud cover, climate change

Citation: Robinson, W. A., R. Reudy, and J. E. Hansen, General circulation model simulations of recent cooling in the east-central United States, *J. Geophys. Res.*, *107*(D24), 4748, doi:10.1029/2001JD001577, 2002.

1. Introduction

[2] During the past half-century, while Earth's climate has warmed, surface air temperatures in the east-central United States have not. Figure 1 shows surface air temperature anomalies averaged over the decade 1988 to 1997 relative to the 1951 to 1980 thirty-year mean. The data and analysis are those described by *Hansen et al.* [2001] (updated from *Hansen et al.* [1999]). Temperatures cooled in the southern plains and warmed slightly elsewhere east of the Rockies. In contrast, the globally averaged terrestrial temperature anomaly for this same decade is 0.35°C.

[3] Regional decreases in surface temperatures have led to suggestions that cooling, in opposition to global warming, might continue. Temperatures in Illinois cooled between the middle and latter part of the twentieth century, leading *Changnon et al.* [1997] to write "The trend towards lower temperatures over the past few decades is so strong and well established that one scenario must be a continuation of the trend towards lower temperatures."

[4] To determine if a continued absence of warming, in the face of expected global increases in temperature, is indeed, likely, it is necessary to understand why it has occurred in the past. There are at least three possible explanations:

1. It could be a direct response to anthropogenic climate forcing. Aerosols, primarily sulfate, are a likely culprit. *Charlson et al.* [1991] show a strong maximum in negative radiative forcing over the eastern half of the United States due to the direct effect of sulfate aerosol, and a more recent calculation by *Penner et al.* [1998] finds an even stronger negative forcing, even though they include the warming influence of carbonaceous aerosol. For anthropogenic aerosol to explain the recent absence of warming, it is necessary that the magnitude of aerosol forcing has

0148-0227/02/2001JD001577$09.00

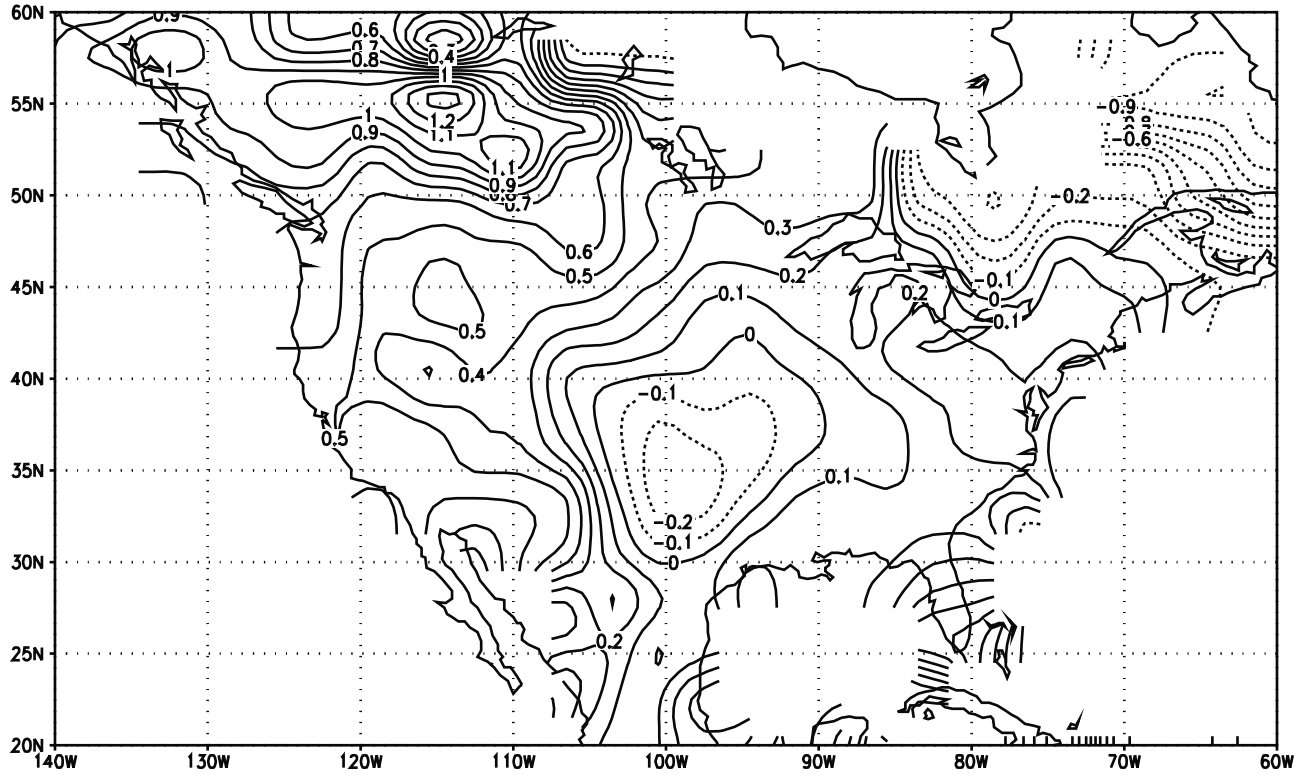

Figure 1. Observed annually averaged surface-temperature anomalies (°C) for the period 1988–1997, with respect to the 1951–1980 thirty-year mean. The contour interval is 0.1°C, and negative contours are dashed.

increased over time. Sulfur emissions and atmospheric loading over the United States have, however, decreased in recent decades, a consequence of policies designed to reduce acid rain [e.g., *Lynch et al.*, 1996].

2. The regional lack of warming could result from internal variability in the climate system. Regional temperature variations could, in this case, be considered a superposition of anthropogenic global warming and regional, internally driven, fluctuations.

3. The absence of warming could be an indirect response to anthropogenic global warming.

[5] Here we present results from a set of retrospective GCM ensemble simulations. The disadvantage of using a GCM to address this problem is that the model is an imperfect representation of nature. The advantage, however, is that we can perform ensembles of simulations with the model, greatly increasing our confidence in any connections that are found between ocean temperatures and the atmospheric climate.

[6] GCM ensembles in which the atmospheric model is forced by the observed evolution of sea-surface temperatures (SST) in the tropical Pacific ocean produce cooling in the east-central United States, regardless of what external climate forcings are included. In contrast, ensembles that do not include the observed evolution of SST invariably fail to produce such cooling. Furthermore, in the ensembles with imposed ocean temperatures, fluctuations in east-central U.S. temperatures are associated with interdecadal variability in tropical Pacific SST. To the extent that they are relevant to nature, these model results support the second or third explanations above, that the observed absence of warming in the east-central United States need not be a direct consequence of anthropogenic climate forcing.

[7] In the next section, we describe the data and simulations used in this study. Section 3 presents an overview of the results and examines the processes that connect east-central U.S. cooling in the model to tropical Pacific SST. Section 4 includes a summary of the results, comparisons with observations, and a discussion of remaining questions.

2. Data, Model, and Simulations

[8] Most of our experiments use a model atmosphere forced by observed varying or climatological SST. The atmospheric model is that used in a previous set of similar experiments [*Hansen et al.*, 1997]. This is a global atmospheric model with a comprehensive set of physical parameterizations. It is a descendent of GISS model II [*Hansen et al.*, 1983] but with significant improvements in its resolution and parameterizations. The present version is run at a horizontal resolution of 4° of latitude by 5° of longitude, and has twelve levels. The model differs from that of *Hansen et al.* [1997] in the addition of three levels in the lower stratosphere. Imposed observed SSTs are taken from the HadISST1 data set [*Rayner et al.*, 1996; *Rayner*, 2000]. All model experiments with imposed SST are carried out as five member ensembles, We also refer to experiments in which the atmospheric model is coupled to an ocean model that predicts SST using the "Q-flux" technique, described by *Hansen et al.* [1988]. In the Q-flux model, the horizontal transport of heat by ocean currents, as opposed to the SST, is held fixed.

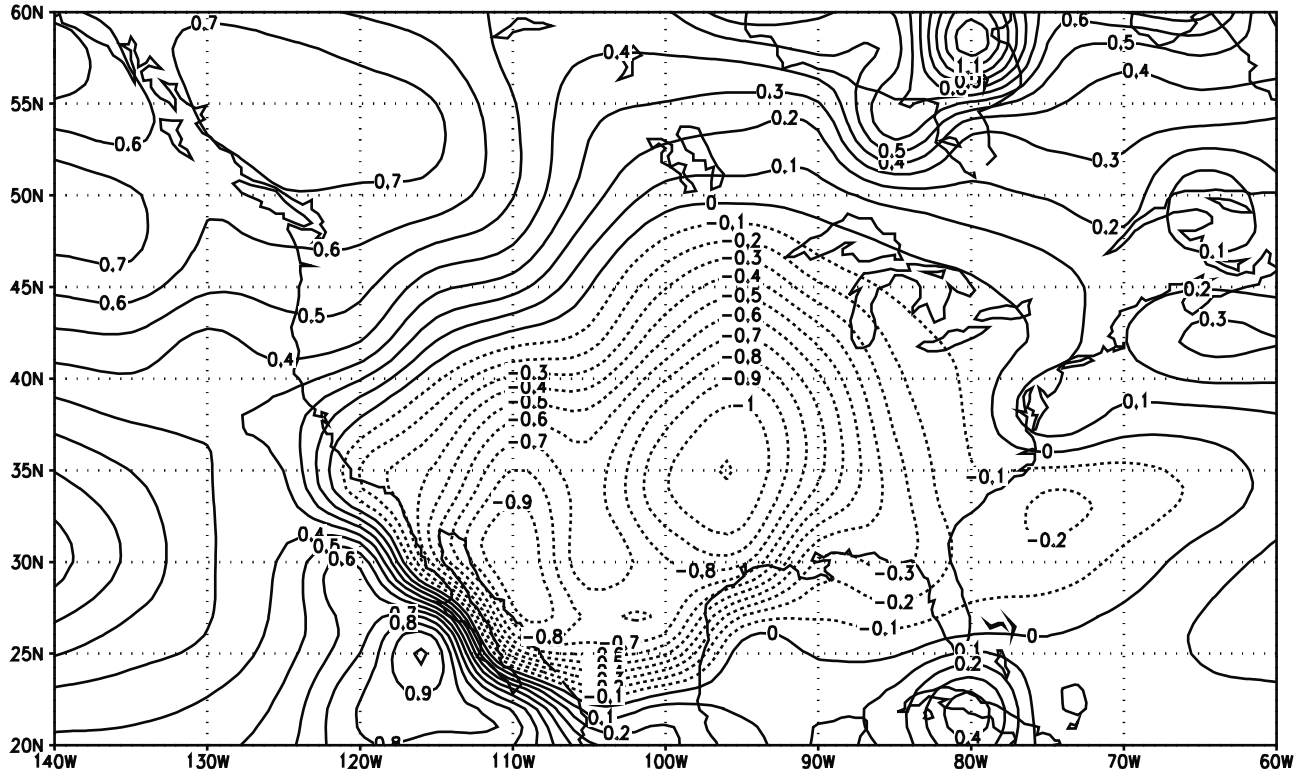

Figure 2. Annual and ensemble average surface-temperature anomalies for the last ten years (1988–1997) of the GOGA ensemble, with respect to the mean of the first thirty years (1951–1980). The contour interval is 0.1°C, and negative contours are dashed.

[9] We focus on four experiments in which all external radiative forcings of the climate, greenhouse gases, solar irradiance, and aerosols, are held fixed at 1950 levels. These are designated as GOGA (global ocean-global atmosphere), TOGA (tropical ocean), TOGA-Pac (tropical Pacific Ocean) and MOGA (midlatitude ocean). In GOGA, observed time varying SST and sea ice from 1951 to 1997 are imposed throughout the world ocean. In TOGA, observed SSTs are imposed equatorward of 20 N and S, while climatological SST and ice are applied elsewhere. MOGA is complementary to TOGA in that climatological SSTs are imposed in the tropics and the observed time varying SST and ice are imposed elsewhere. In TOGA-Pac observed SST are imposed only within the tropical Pacific Ocean.

3. Results

3.1. Overview

[10] The east-central United States cools in the GOGA ensemble. Figure 2 shows annual and ensemble averaged surface-temperature anomalies for the last ten years of the run (1988–1997) with respect to the mean of the first thirty years (1951–1980). The cooling in the model is much stronger than is observed (Figure 1), and has two maxima. One is in the east-central United States, and the second, not present in the observations, is centered over the Mexican state of Sonora. Cooling in both regions is present in all five members of the ensemble. The strength of the east-central U.S. cooling ranges across the ensemble from 0.5 to 1.8°C, and that of the Sonoran cooling from 0.5 to 1.5°C.

[11] Figure 3 shows the annual cycle of anomalous temperatures for each of the five members of the GOGA ensemble. As in Figure 2, the quantity plotted is the difference in the temperature of the final 10 years of the run from that of the first 30, but now taken month by month and averaged over a broad region of the United States east of the

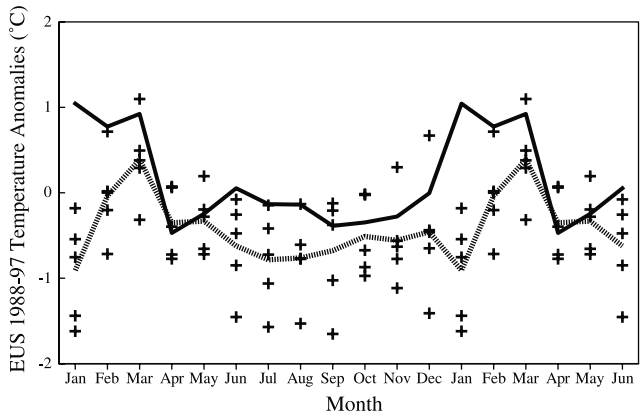

Figure 3. The difference in the temperature of the final 10 years of each GOGA run from that of the first 30, averaged over the EUS box, from 75 to 105°W and from 30 to 45°N. One and one-half annual cycles are shown. The crosses show the individual members of the GOGA ensemble, the dashed curve shows the ensemble average, and the solid curve shows the observed anomalies.

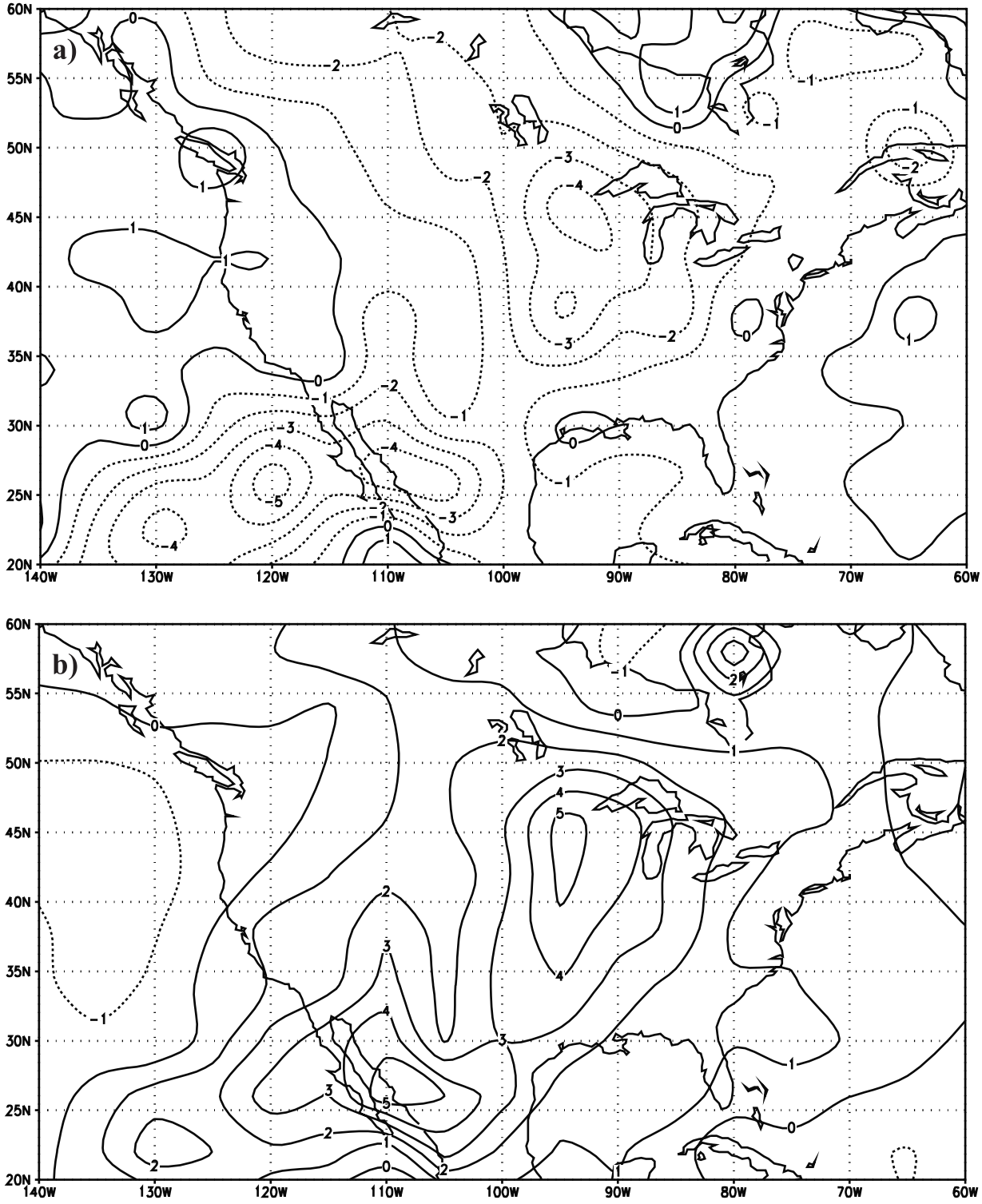

Figure 4. Annual and ensemble average anomalies or the last ten years (1988–1997) of the GOGA ensemble, with respect to the mean of the first thirty years (1951–1980). (a) Net downward radiation at the top of the atmosphere (W m-2). (b) Low cloud amount (%). The contour interval is 1 W m-2 in Figure 4a and 1% in Figure 4b, and negative contours are dashed.

Figure 5. (opposite) Annual and ensemble average surface temperature anomalies for the last ten years (1988–1997) of GCM ensembles, with respect to the mean of the first thirty years (1951–1980): (a) TOGA, (b) TOGA-Pac, and (c) MOGA ensemble. The contour interval is 0.1°C, and negative contours are dashed.

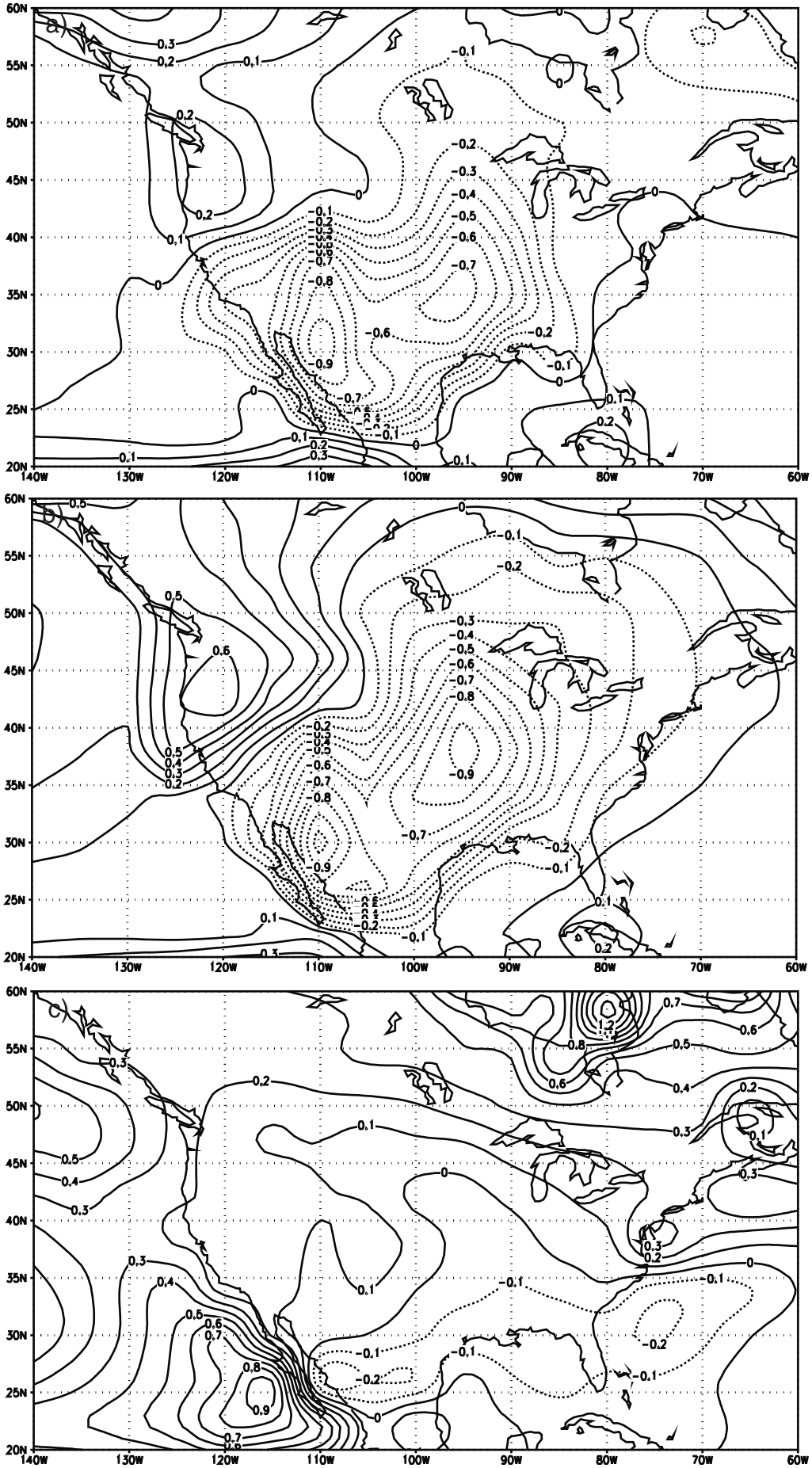
a)
b)
c)
60N
55N
50N
45N
40N
35N
30N
25N
20N
140w
130w
120w
110w
100w
90w
80w
70w
60w

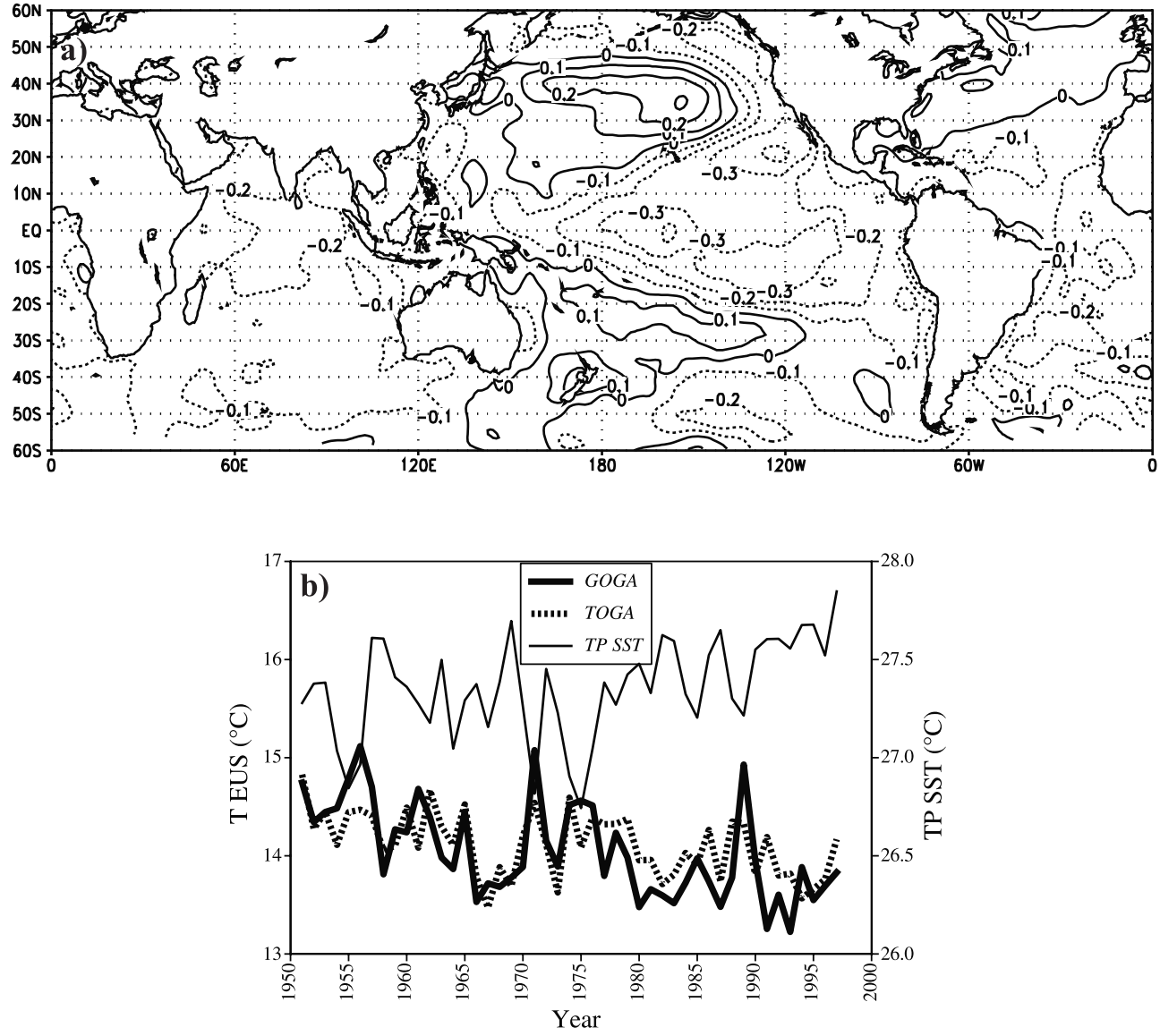

Figure 6. (a) Regressions of annually averaged SST against GOGA ensemble-average EUS surface temperatures. The contour interval is 0.1°C, and negative contours are dashed. (b) Time series of tropical Pacific SST (TP SST, thin solid curve), EUS surface temperatures in the GOGA (thick solid curve), TOGA (dashed curve), and TOGA-Pac (thick dashed curve) ensembles.

Rockies, from 75 to 105°W and from 30 to 45°N (this "box" is henceforth denoted EUS). All five members of the ensemble show cooling in January and from June through September. The observed anomalies for the same region (the solid curve in Figure 3) are positive in January through March and in June, and are negative throughout the remainder of the year. Except in January, when all five ensemble members show cooling, while the observations show strong warming, the observed anomalies are within or near the top of the range of modeled temperature anomalies.

[12] Determining the source of cooling in the model may contribute to our understanding of the observed regional temperature trend, specifically its departure from global warming. The model cooling is radiatively driven. Figure 4a shows anomalies, for 1988–1997 relative to 1951–1980, in net downward radiation, shortwave plus longwave, at the top of the atmosphere. These anomalies are driven by an increase in reflected and backscattered solar radiation and are opposed by modest decreases in the outgoing longwave radiation. If, on the other hand, the cooling were driven by thermal advection, then changes in net radiative heating should oppose the changes in surface temperature. Averaged over the EUS region, the 1988–1997 anomalies are −.47°C in surface temperature and −1.6 W m^{-2} in net downward radiation. The same association between net downward radiation and surface temperature is found for the model's interannual variability. In the EUS box, net top of the atmosphere radiation is strongly correlated with year-to-year variations in temperature (r = 0.81). Since longwave cooling tends to increase with the surface temperature, this implies a stronger relationship between the surface temperature and the net shortwave radiation, and their correlation is 0.87.

[13] The variations in net solar heating are controlled by variations in cloud amount. Figure 4b shows 1988–1997

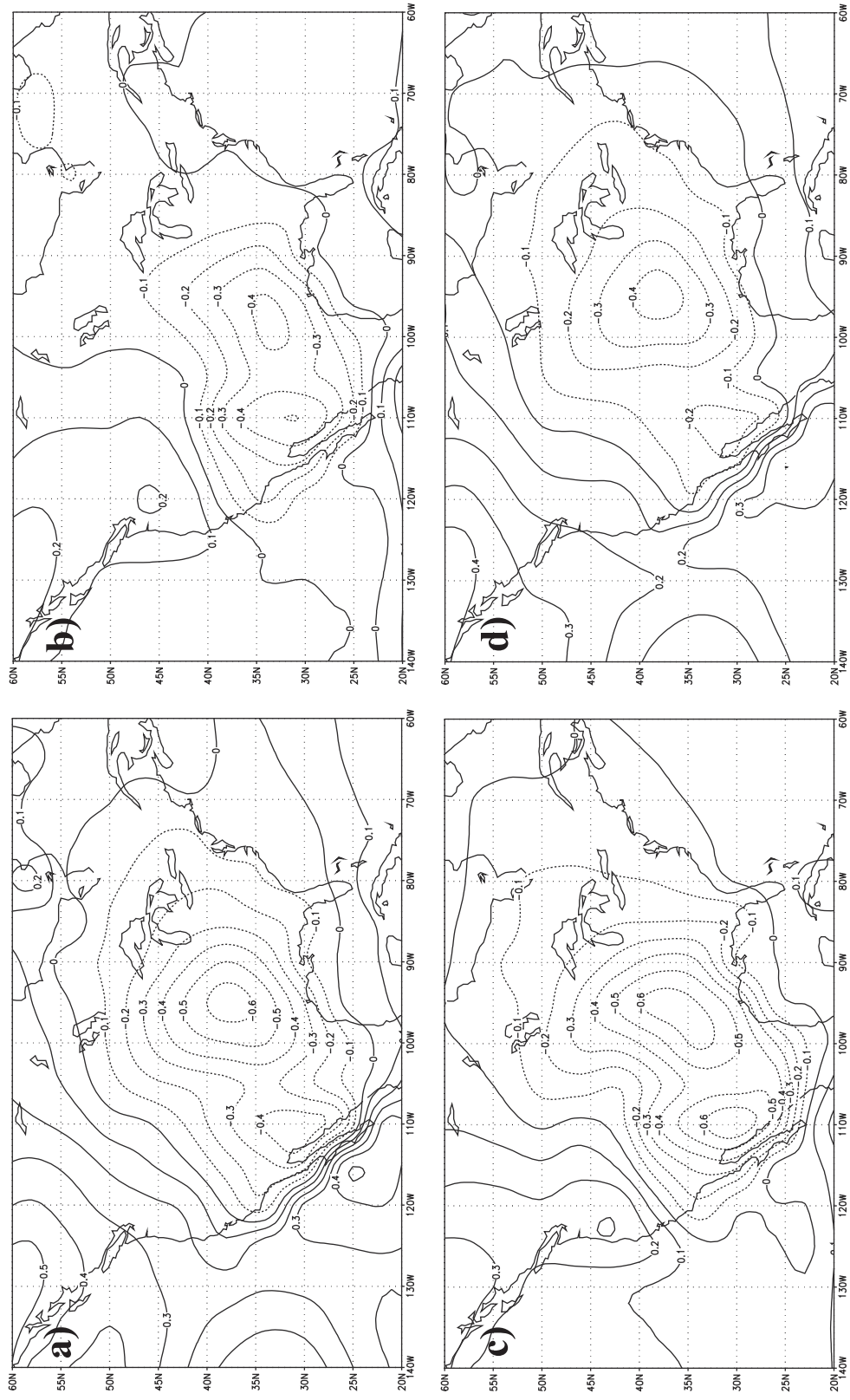

Figure 7. Annual and ensemble average surface temperatures (°C) in the (a) GOGA, (b) TOGA, and (c) TOGA-Pac ensembles regressed against the time series of annually averaged TP SST. Panel (d) is the same as (a) but with the linear trend removed from the TP SST time series. The contour interval is 0.1°C, and negative contours are dashed.

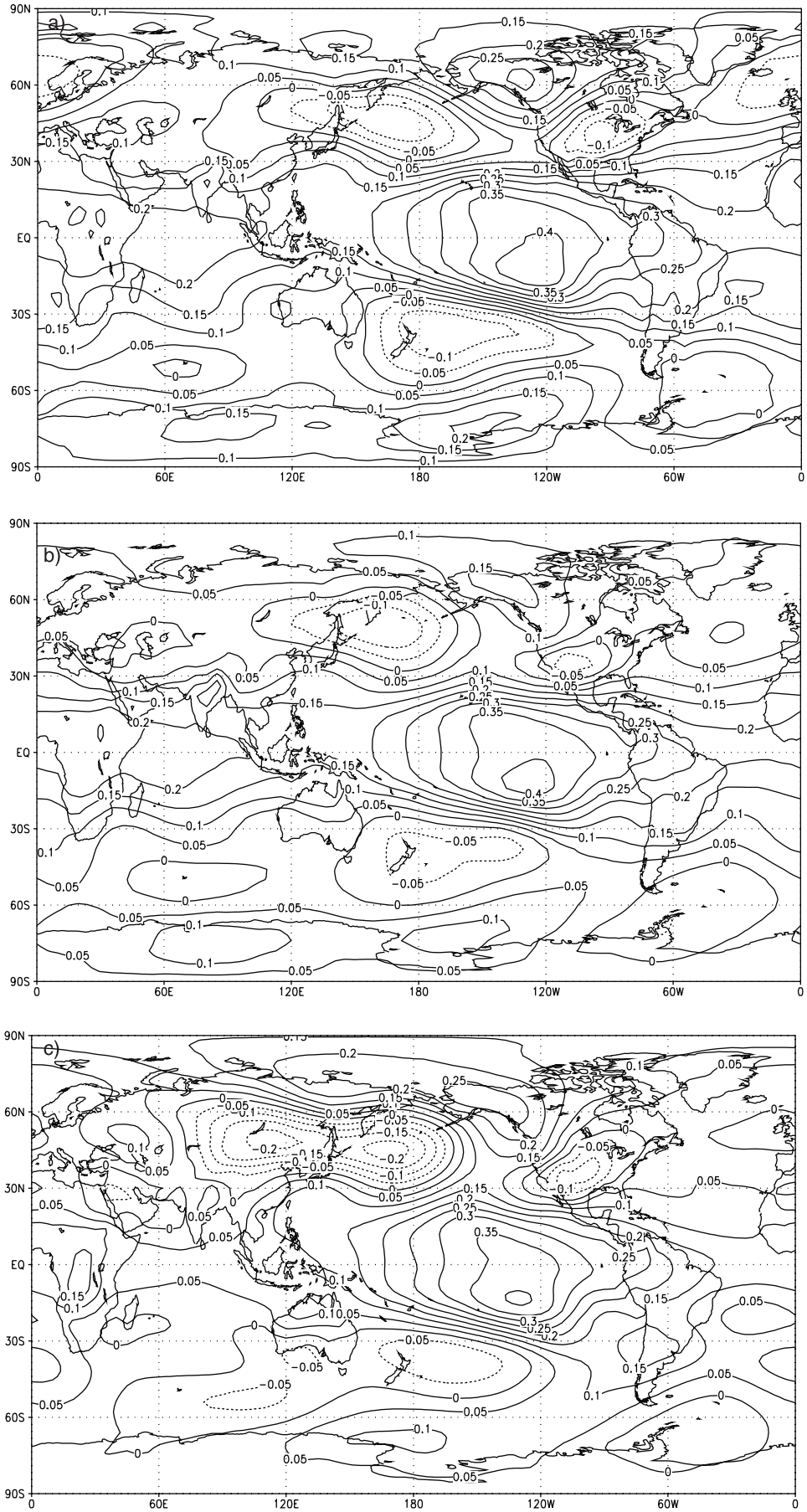
a)
b)
c)
90N
60N
30N
EQ
30S
60S
90S
0
60E
120E
180
120W
60W

anomalies, relative to 1951–1980, in the percent coverage of low cloud. The average anomaly over EUS is +2.6 %. The pattern, with a change of sign, is very similar to that in Figure 4a. The correlation between the year-to-year variations in annually and ensemble averaged low-cloud amount and surface temperature, for the EUS box, is −.88.

[14] Some insight into the source of increased cloud cover and, therefore, cooling comes from comparing results from the four different ensembles, GOGA, TOGA, TOGA-Pac, and MOGA. Figure 5 shows the ensemble-averaged temperature anomalies averaged over the last 10 years of the TOGA, TOGA-Pac, and MOGA ensembles. When only tropical SST are imposed (TOGA, Figure 5a) the cooling is similar to that in the GOGA runs (Figure 2), though the east-central U.S. lobe is slightly weaker. When tropical Pacific SSTs are imposed (TOGA-Pac, Figure 5b) nearly all of the cooling in the GOGA ensemble is recovered. In contrast, when only extratropical SSTs are imposed (MOGA, Figure 5c) the cooling is far weaker and is confined to the southern tier of the United States.

[15] The GISS GCM has been used to carry out many additional ensembles of retrospective runs, incorporating various combinations of time-varying radiative forcings, including anthropogenic aerosols and greenhouse gases. It is found that, regardless of what radiative forcing is imposed, east-central U.S. cooling appears only in those runs in which observed SST are imposed in the tropical Pacific.

3.2. Connections With the Tropical Pacific

[16] Comparing the four model ensembles indicates that tropical Pacific SST significantly influences EUS surface temperatures in the GISS GCM. Figure 6a shows the pattern of global SST associated with a positive anomaly of one standard deviation in the ensemble and annually averaged EUS surface temperature. The values displayed in Figure 6a are obtained by standardizing the EUS temperature time series, so that it has zero mean and unit variance, and then regressing annual averages of the SST at every ocean grid point against this series. The resulting pattern has considerable cross- equatorial symmetry in the Pacific. There are low SSTs in a triangle with its apex on the equator in the western Pacific and extending into the subtropics near the coasts of the Americas. Lobes of warm SST appear in the middle latitudes of both hemispheres. Similar SST patterns were found by *Zhang et al.* [1997] to be associated with interdecadal variability in the tropical Pacific. At the same time, the pattern in Figure 6a, with its strong extratropical lobe and its lack of an equatorial maximum, is significantly different from what would be obtained by regression against an index of El Niño, such as the cold tongue index (CTI). The temporal variations of the SST pattern in Figure 6a are readily captured by a simple index of basin-wide tropical Pacific SST. In what follows we use the annually averaged SST averaged over a tropical band between 20 N and 20 S from 130 E to 85 W, denoted TP SST, as a measure of tropical Pacific SST. Regressions of SST against the TP SST index are nearly indistinguishable from Figure 6a. Consistent with the results of Zhang et al. the TP SST time series is very similar to what is obtained by applying a multiyear low-pass filter to the CTI. Statistical relationships similar to those described below are obtained using the CTI, but are weaker. The implication is that, in the GCM, atmospheric conditions over the United States are more responsive to slow ''ENSO-like'' variations in tropical Pacific SST than they are to El Niño itself.

[17] Figure 6b shows the time series of EUS surface temperatures in the GOGA, TOGA, and TOGA-Pac runs, together with that of TP SST. The correlation of TP SST with the GOGA-ensemble average of EUS surface temperature is −.65. A similar correlation, −.68 is obtained from the TOGA-Pac ensemble, and a somewhat lower value, −.45, from the TOGA experiment. The correlations of TP SST with EUS surface temperatures in the individual members of the GOGA ensemble range from −.38 to −.51, with an average value of −.48. In all three ensembles, the ensemble average of EUS low-cloud cover is strongly correlated with TP SST (r = 0.69 in GOGA, 0.61 in TOGA, and0.86 in TOGA-Pac), and the incoming shortwave radiation and net radiative forcing are, consequently, inversely related to TP SST.

[18] The importance of tropical Pacific SST for east-central U.S. temperatures in the GISS GCM is confirmed by examining the temperature patterns associated with fluctuations in TP SST. Figure 7 shows annual and ensemble averaged North American surface temperatures regressed against TP SST for the GOGA, TOGA, and TOGA-Pac ensembles. These patterns, computed in a manner analogous to that described for Figure 6a, are those that would appear in association with a one standard deviation positive anomaly in TP SST. They are very similar to those displayed in Figures 2 and 5.

[19] The possibility remains that the apparent relationship between North American surface temperature and tropical Pacific SST is a consequence of independent trends in each quantity, without any causal link. Figure 7d, however, argues against this. The calculation is the same as for Figure 7a, but now the linear trend (+.08°C/decade) is removed from TP SST before the regression is performed. The pattern is nearly the same as that in Figure 7a, with a slight reduction in its amplitude. Thus most of the statistical relationship between tropical Pacific SST and North American surface temperatures derives from their variability, as opposed to their fifty-year trends.

[20] Regressions of net downward radiation and cloud cover against TP SST (not shown) show a similar result, yielding patterns similar to those in Figure 4. A consistent picture emerges, in which, in the GISS GCM, elevated tropical Pacific SST, especially on multi-year timescales, causes increased cloud cover over the east-central United States, thereby reducing surface temperatures. Further analyses reveal that the increase in cloudiness and subsequent surface cooling may be viewed as a local enhancement of the model's global thermal response to tropical warming.

Figure 8. (opposite) Annual and ensemble average tropospheric temperatures (°C), defined as the GCM simulation of the temperature derived from MSU channel 2 from the (a) GOGA, (b) TOGA, and (c) TOGA-Pac ensembles regressed against TP SST. The contour interval is 0.05°C, and negative contours are dashed.

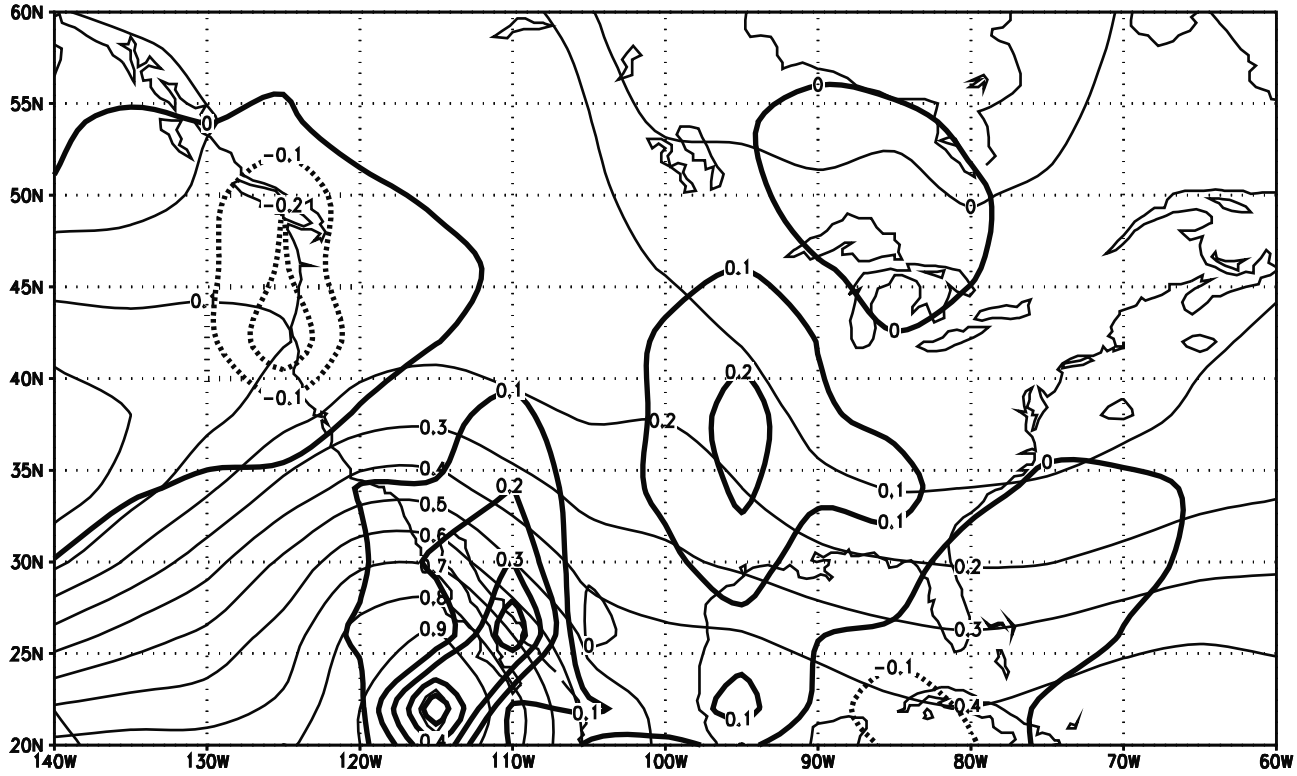

Figure 9. Annual and ensemble average precipitable water (mm, thin contours) and precipitation (mm/day, thick contours), from the GOGA ensemble, regressed against TP SST. The contour interval is 0.1 mm, and reduced precipitation is indicated by dashed contours.

Figure 8 shows the global pattern of tropospheric temperatures associated with warm tropical Pacific SST in the GOGA, TOGA, and TOGA-Pac ensembles. These maps are obtained by regressing annual and ensemble averaged tropospheric temperatures (defined here as the GCM simulation of the temperature that would be measured by channel 2 of the Microwave Sounding Unit) against the annual average of TP SST. In all three experiments, warm tropical Pacific SST are associated with tropospheric warmth throughout the tropics, and with wavy broken bands of weaker cooling in middle latitudes. Similar patterns were found in observations by *Yulaeva and Wallace* [1994]. This global pattern in tropospheric temperatures can be understood as an eddy-mediated dynamical consequence of tropical warming [*Robinson*, 2002]. Very similar patterns of tropical warming with a wavy band of cooling across the North Pacific and North America are found in both 500–1000 hPa and 300–500 hPa thickness temperatures (not shown), with magnitudes similar to those in Figure 8. Thus, over the east-central United States, the thermal response to a one standard deviation increase in tropical Pacific SST is surface cooling of more than 0.5°C (Figure 7a) beneath a deep tropospheric cooling of 0.1 to 0.2°C.

[21] Away from the surface, the global response of the GCM to tropical warmth is an increase in the equatorward temperature gradient across 30°N, the latitude of the U.S. Gulf Coast. Warming of the atmosphere over the Gulf leads to an increase in specific humidity. Figure 9 shows the column precipitable water vapor for the GOGA ensemble regressed against TP SST. Tropical warmth is associated with an increase in specific humidity over the Gulf that extends northward, with reduced strength, over most of North America. There is also a strong increase in precipitable water over the locally warm SSTs off Baja California. The heavy contours in Figure 9 show the anomalous precipitation (similarly computed by regression against TP SST) associated with tropical warmth. The regions of increased precipitation correspond to the regions of increased cloudiness shown in Figure 4.

[22] The increased precipitable water and reduced tropospheric temperature over the Central United States imply that when the tropical Pacific SST is warm, the relative humidities over the east-central United States are higher and clouds are more likely to form. Consider an unsaturated air parcel originating in the lower troposphere over the Gulf of Mexico or the Caribbean. This parcel may be carried poleward, on an isentropic trajectory, over North America, either by the mean circulation around the Atlantic subtropical high, which in the GCM warm season extends westward to 100°W, or by poleward advection in the warm sector of an extratropical cyclone. The parcel will become saturated (reach its lifting condensation level) and contribute to stratiform cloud cover further south if its initial humidity is greater and/or the upward slope if its trajectory is greater. The latter condition can be satisfied by an increase in the strength of the meridional temperature gradient. It appears that both conditions for increased cloud cover are present in the GCM when the tropical Pacific is warm, but the daily model output required to verify that these are the sources of increased cloud cover is not available.

[23] We attribute increased east-central U.S. cloudiness and the subsequent decrease in surface temperature to a local manifestation of a global response to tropical warmth, as opposed to the Rossby wave train patterns typically associated with the midlatitude response to El Niño [*Horel and Wallace*, 1981]. The GCM generates a wave-train response to warm tropical Pacific SST, but this response is confined to the cold season. Figure 10 shows the regression of 500 hPa geopotential height anomalies in the GOGA ensemble against the annually averaged TP SST, for December, January, and February (Figure 10a) and for June, July, and August (Figure 10b). A wave train is evident in winter, but absent in summer. In contrast, the global response in tropospheric temperature is present throughout the year. Figure 11a shows zonally averaged tropospheric temperatures from the GOGA ensemble regressed against TP SST. Tropical warmth and the resulting enhanced subtropical temperature gradient are evident in all months. Midlatitude cloud cover and surface temperature, averaged from 30 to 45°N and regressed against TP SST, show that increased cloudiness and surface cooling between 80 and 120°W, similarly occur throughout the year (Figures 11b and 11c), This lack of seasonality is consistent with the global response of tropospheric temperatures to tropical warming, but is inconsistent with the tropically generated Rossby wave train.

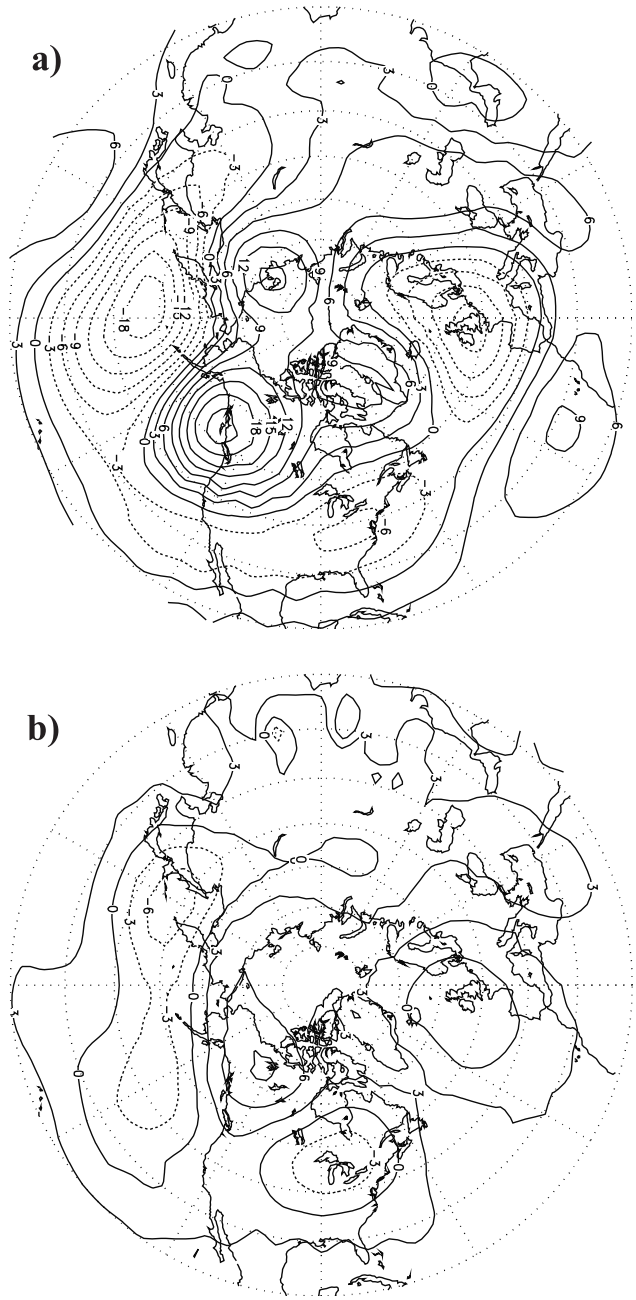

Figure 10. Geopotential height anomalies at 500 hPa, from the GOGA ensemble, regressed against TP SST, for (a) December, January and February, and (b) June, July, and August. The contour interval is 3 m, and negative contours are dashed.

4. Summary and Discussion

[24] We examine a set of retrospective ensemble GCM runs, focusing on the causes of cooling in the east-central United States over the second half of the twentieth century. The GCM, when forced by observed, time varying, SST, but using fixed atmospheric composition and solar irradiance, produces cooling in this region. The cooling in the GCM is robust. It occurs in all members of the ensemble, and in all simulations in which time varying observed tropical Pacific SSTs are imposed regardless of what radiative forcing is used. Cooling fails to occur in any simulation in which the time varying tropical SST is *not* imposed.

[25] The proximate cause of the cooing is decreased net insolation due to an increase in cloud cover. In all experiments with imposed tropical Pacific SST, fractional coverage of low cloud in the model is well correlated with these ocean temperatures. The local surface cooling of the east-central United States is, moreover, embedded in a global-scale tropospheric response. Tropospheric warming associated with warm tropical Pacific SST is confined to the tropics and subtropics, with regions of cooling in middle latitudes. Thermodynamic arguments suggest that the increased EUS cloud cover could result from elevated temperatures and specific humidities in the subtropics south of the United States and from increased tropospheric thermal gradients across the Gulf Coast.

[26] No other land area shows the same robust surface cooing in the GCM ensembles, as does the east-central United States. Similarly, no other region shows a strong association between cloud cover and tropical Pacific SST. This region appears to be unique, in that tropical Pacific warming drives both an increase in tropospheric water vapor and a decrease in tropospheric temperatures.

[27] Does the GCM faithfully mimic nature in producing this response to tropical SST? First, observations suggest that cooling temperatures in the eastern United States, relative to the rest of the globe, have been accompanied by increasing trends in water vapor and cloud cover, as is shown in Figure 12. The water vapor data are quality-controlled surface to 500 hPa values of precipitable water obtained from radiosondes [*Ross and Elliot*, 2001]. The anomalies shown in Figure 13 correspond to the average values over an "eastern U.S." box that extends from 15 to 45°N latitude and from 60 to 100°W longitude. The cloud data are averages over 70 U.S. surface observing stations

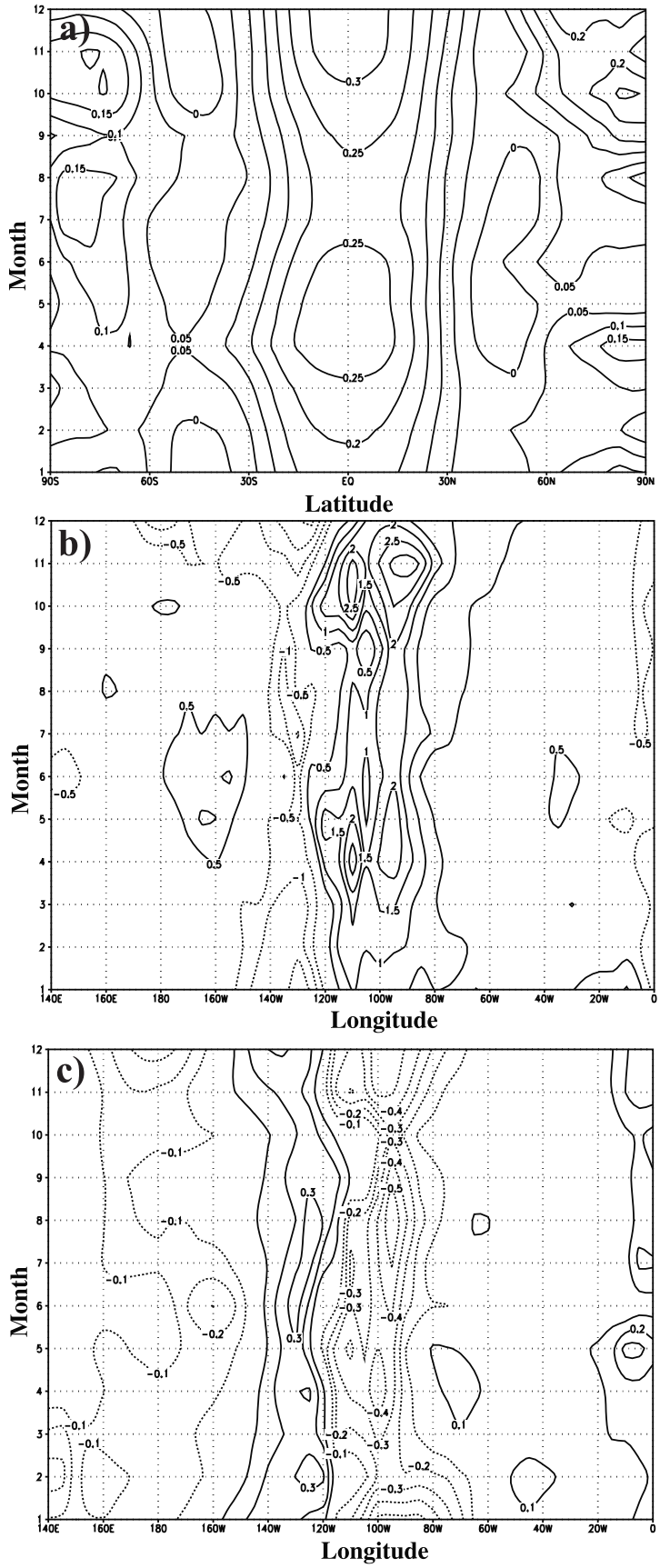

Figure 11. Regressions against TP SST in the GOGA ensemble of (a) zonally averaged tropospheric temperature (°C), (b) low-cloud cover (%) averaged between 30 and 45°N, and (c) surface temperature (°C) averaged between 30 and 45°N.

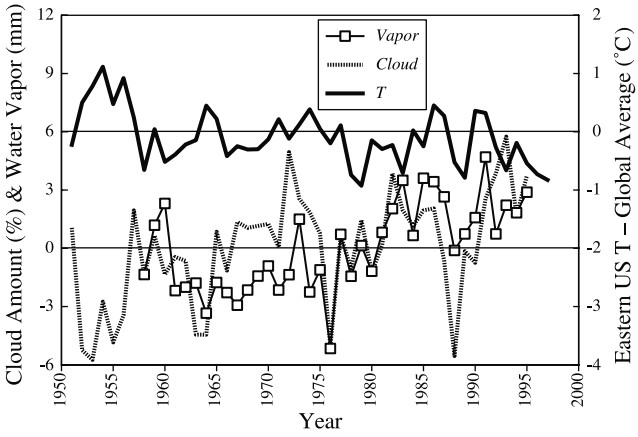

Figure 12. Observed anomalies over the eastern United States in surface air temperature (°C, solid curve), cloud amount (%, thick dashed curve), and precipitable water (mm, open squares). Surface temperatures are averaged over the EUS box, and the global mean temperature anomaly for each year is subtracted. Cloud amounts are averages of opaque cloud cover over approximately 70 observing stations east of the Rocky Mountains, and precipitable water is averaged over radiosonde stations between 15 and 45°N latitude and between 60 and 100°W longitude.

east of the Rocky Mountains, prepared from hourly reports of opaque cloud cover. The surface temperatures are deviations of the temperature anomalies in the EUS box from the globally averaged anomaly, calculated using the same data as in Figure 1.

[28] Figure 12 shows that in the observations, eastern U.S. water vapor and cloud cover have increased, and they tend to vary together (r = 0.50), though it should be noted that these series represent averages over different regions. Similar positive trends in cloud cover are shown by *Dai et al.* [1999]. It is also consistent with the GCM results that eastern U.S. precipitable water is well correlated (r = 0.55) with TPAC SST. The relationship between cloud cover and surface temperature is weaker (r = −0.33), as is the relationship between TPAC SST and cloud cover (r = 0.38).

[29] A recent observational analysis of the surface moisture and energy budgets in the Mississippi basin [*Milly and Dunne*, 2001], supports the present findings of decreasing insolation and increasing precipitation over the second half of the twentieth century. They, however, find a statistical connection between these changes and the North Atlantic Oscillation (NAO), while, in the GCM, the source of these variations in tropical Pacific SST is clear. In the GCM, warm tropical SST and cool east-central U.S. temperatures are associated with a modest decrease in the NAO, especially during the winter.

[30] The association between surface temperature and low-cloud in the EUS region is very strong, perhaps too strong, in the model, even in the absence of strong SST variations. In a single fifty-year simulation using the Q-flux ocean, and with fixed radiative forcing, there is little variation in SST; the variability in tropical Pacific SST is roughly one tenth of that observed. The variability in EUS surface temperatures, however, is nearly as great as any member of the GOGA ensemble, and these temperatures have a strong inverse correlation with low-cloud cover (r = −.73). The interannual variability of the surface temperature in this run is especially strong in the EUS region, as well as in other regions, such as Australia and southern Africa where surface temperatures and low cloud amounts are strongly and negatively correlated. Thus the response of the GCM to varying Pacific SST can be seen as the stimulation by tropical SST of one of the model's internal modes of variability. That surface temperature-low cloud coupling may be overly robust in the GCM is supported by the fact that the interannual variability in EUS surface temperatures, as measured by their standard deviation, is half again as large in the model with the Q-flux ocean as in observations.

[31] A final question is whether there is any observational evidence supporting a connection between tropical Pacific Ocean SST and east-central U.S. surface temperatures. Figure 13 shows annually averaged Illinois surface temperatures [*Changnon et al.*, 1997] and values of the cold-tongue index (CTI), both smoothed by a nine-year running mean. The CTI is calculated from the Comprehensive Ocean Data Set (COADS) by Dr. Todd Mitchell, and is available at http://tao.atmos.washington.edu. It is obtained by taking the average of SST anomalies over the region within six degrees of the equator between 90 and 180°W longitude, and then subtracting the globally averaged SST. When smoothed, as in Figure 13, the CTI is well correlated with the TP SST series over the period 1950–1997 (r = 0.89). The Illinois temperatures (unsmoothed) are similarly well correlated with the EUS T time series (r = .93) over the same period. Two features of Figure 13 are noteworthy. First, there is a tendency for temperatures in Illinois and the tropical Pacific to vary in opposition on interdecadal timescales (r = −.49). Secondly, there is a period early in the twentieth century when the tropical Pacific was warm and Illinois was cool. It is unlikely that this earlier tropical warming was anthropogenic. From this record it is, therefore, plausible that recent fluctuations in tropical ocean temperatures, along with their possible influence on U.S. temperatures, are manifestations of internal variability in the climate system. In this case, the Illinois temperature record could be interpreted as a superposition of mutually independent influences from internal climate variability and anthropogenic warming. If so, we may expect that even-

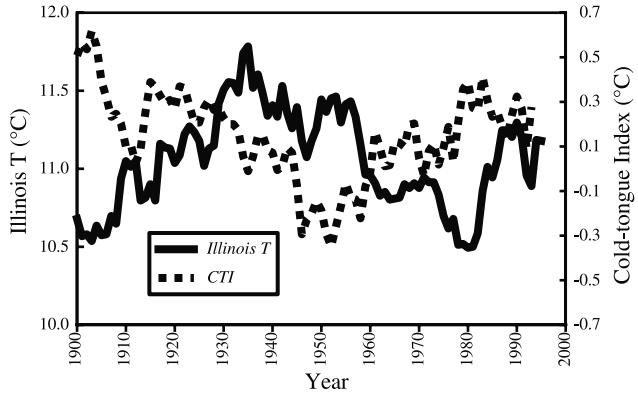

Figure 13. Illinois temperatures (solid) and the cold-tongue index (dashed), both smoothed by a nine-year running mean.

tually internal variations in the tropical Pacific will swing the other way, and that warming in the east-central United States will catch up with the rest of the globe.

[32] On the other hand, *Trenberth and Hoar* [1996, 1997] argue that the intense and prolonged warmth of the tropical Pacific in the 1990's was unprecedented, and, therefore, likely a consequence of anthropogenic climate change. This view was disputed by *Rajagopalan et al.* [1997]. If Trenberth and Hoar are correct, and if the connection between tropical Pacific SST and east-central U.S. temperatures proposed here is valid, then the cooling of the east-central United States relative to the rest of the globe would be an indirect manifestation of global warming. Resolving this issue is far beyond the scope of the present work. The present results suggest, however, that variations in tropical Pacific SST are important for U.S. climate over the same time scales relevant to anthropogenic climate change. Meaningful statements about the regional impacts of anthropogenic climate change on the United States must, therefore, be preceded by an understanding of how anthropogenic climate change will influence the tropical Pacific Ocean.

[33] **Acknowledgments.** For Figure 12, Rebecca Ross of NOAA's Air Resources Laboratory kindly provided numerical values of precipitable water, and Kenneth Kunkel of the Illinois State Water Survey graciously provided the cloudiness data. Helpful comments from three anonymous reviewers are gratefully acknowledged. WR's involvement in this work was supported by the National Oceanic and Atmospheric Administration, through grant NA76GP0323.

References

Changnon, S. A., D. Winstanley, and K. E. Kunkel, An investigation of historical temperature and precipitation data at climate benchmark stations in Illinois, *Circ. 184*, Ill. State Water Surv., Champaign, Ill., 1997.

Charlson, R. J., J. Langner, H. Rodhe, C. B. Leovy, and S. G. Warren, Perturbation of the Northern Hemisphere radiative balance by backscattering from anthropogenic sulfate aerosols, *Tellus, Ser. AB*, *43*, 152–163, 1991.

Dai, A., K. E. Trenberth, and T. R. Karl, Effects of clouds, soil moisture, precipitation, and water vapor on diurnal temperature range, *J. Clim.*, *12*, 2451–2473, 1999.

Hansen, J., G. Russell, D. Rind, P. Stone, A. Lacis, S. Lebedeff, R. Ruedy, and L. Travis, Efficient three-dimensional global models for climate studies: Models I and II, *Mon. Weather Rev.*, *111*, 609–662, 1983.

Hansen, J., I. Fung, A. Lacis, D. Rind, Lebedeff, R. Ruedy, G. Russell, and P. Stone, Global climate changes as forecast by Goddard Institute for Space Studies three-dimensional model, *J. Geophys. Res.*, *93*, 9341–9364, 1988.

Hansen, J., et al., Forcings and chaos in interannual to decadal climate change, *J. Geophys. Res.*, *102*, 25,679–25,720, 1997.

Hansen, J., R. Ruedy, J. Glascoe, and M. Sato, GISS analysis of surface temperature change, *J. Geophys. Res.*, *104*, 30,997–31,022, 1999.

Hansen, J., R. Ruedy, M. Sato, M. Imhoff, W. Lawrence, D. Easterling, T. Peterson, and T. Karl, A closer look at United States and global surface temperature change, *J. Geophys. Res.*, *106*, 23,947–23,963, 2001.

Horel, J. D., and J. M. Wallace, Planetary-scale phenomena associated with the southern oscillation, *Mon. Weather Rev.*, *109*, 813–829, 1981.

Lynch, J. A., V. C. Bowersox, and J. W. Grimm, Trends in precipitation chemistry in the United States, 1983–94: An analysis of the effects in 1995 of Phase I of the Clear Air Act Amendments of 1990, Title IV, *U.S. Geol. Surv. Open File Rep. 96-0436*, Reston, Va., 1996.

Milly, P. C. D., and K. A. Dunne, Trends in evaporation and surface cooing in the Mississippi River basin, *Geophys. Res. Lett.*, *28*, 1219–1222, 2001.

Penner, J. E., C. C. Chuang, and K. E. Grant, Climate forcing by carbonaceous and sulfate aerosols, *Clim. Dyn.*, *14*, 839–851, 1998.

Rajagopalan, B., U. Lall, and M. A. Cane, Anomalous ENSO occurrences: an alternative view, *J. Clim.*, *10*, 2351–2357, 1997.

Rayner, N. A., HADISST1 sea ice and sea surface temperature data files, Hadley Cent. for Clim. Predict. and Res., UK Met Office, Bracknell, UK, 2000.

Rayner, N. A., E. B. Horton, D. E. Parker, C. K. Folland, and R. B. Hackett, Version 2.2 of the global sea-ice and sea surface temperature data set, 1903–1994, *Clim. Res. Tech. Note 74*, Hadley Cent. for Clim. Predict. and Res., UK Met Office, Bracknell, UK, 1996.

Robinson, W. A., On the midlatitude thermal response to tropical warmth, *Geophys. Res. Lett.*, *29*(8), 1190, doi:10.1029/2001GL014158, 2002.

Ross, R. J., and W. P. Elliot, Radiosonde-based Northern Hemisphere tropospheric water vapor trends, *J. Clim.*, *14*, 1602–1612, 2001.

Trenberth, K. E., and T. J. Hoar, The 1990–1995 El Niño-Southern Oscillation event: Longest on record, *Geophys. Res. Lett.*, *23*, 57–60, 1996.

Trenberth, K. E., and T. J. Hoar, El Niño and climate change, *Geophys. Res. Lett.*, *24*, 3057–3060, 1997.

Yulaeva, E., and J. M. Wallace, The signature of ENSO in global temperature and precipitation fields derived from the microwave sounding unit, *J. Clim.*, *7*, 1719–1736, 1994.

Zhang, Y., J. M. Wallace, and D. S. Battisti, ENSO-like interdecadal variability: 1900–93, *J. Clim.*, *10*, 1004–1020, 1997.

W. A. Robinson, Department of Atmospheric Sciences, University of Illinois at Urbana-Champaign, 105 South Gregory Street, Urbana, IL 61801, USA. (robinson@atmos.uiuc.edu)

J. E. Hansen and R. Reudy, NASA/Goddard Institute for Space Studies, 2880 Broadway, New York, NY 10025, USA. (jhansen@giss.nasa.gov; cdrar@ipcc2.giss.nasa.gov)